Yan Zhang, Xiaonan Li, Zhenhu Cao, Zhengping Fang, T. Richard Hull, and Anna A. Stec
Synthesis of Zinc Phosphonated Poly(ethylene imine) and Its Fire-Retardant Effect in Low-Density Polyethylene
Industrial & Engineering Chemistry Research **2015** *54* (13), 3247-3256

Synthesis of zinc phosphonated poly(ethylene imine) and its fire retardant effect in low density polyethylene

Yan Zhang[1,3], Xiaonan Li[1], Zhenhu Cao[2], Zhengping Fang[1,2*] , T Richard Hull[3*], Anna A. Stec[3]

1 Lab of Polymer Materials and Engineering, Ningbo Institute of Technology, Zhejiang University, Ningbo 315100, China
2 MOE Key Laboratory of Macromolecular Synthesis and Functionalization, Department of Polymer Science and Engineering, Zhejiang University, Hangzhou 310027, China
3 Centre for Fire and Hazards Science, University of Central Lancashire, Preston PR1 2HE, UK
E-mail: zpfang@zju.edu.cn, trhull@uclan.co.uk

Abstract

A novel oligomeric intumescent fire retardant chelate, zinc phosphonated poly(ethylene imine) (Zn-PEIP), with a changeable Zn^{2+} loading, was synthesized. The chemical structure of Zn-PEIP was confirmed by FTIR, ^{13}C NMR and ^{31}P NMR spectroscopy. The thermal behavior and fire retardancy of low density polyethylene (LDPE) containing 25 wt% Zn-PEIPs with different amounts of Zn^{2+} were investigated by thermogravimetric analysis (TGA), limiting oxygen index (LOI) and cone calorimetry. The TGA results showed that higher concentrations of Zn^{2+} improved the thermal stability and increased the residue yield of LDPE. However, the data from the LOI and cone calorimetry showed that there is an optimum concentration of Zn^{2+} for the best fire retardant performance of LDPE. This is ascribed to the high crosslink density resulting from zinc bridges, preventing normal swelling of the intumescent system. The surface morphology of the char was characterized by digital photographs and scanning electron microscopy (SEM). This confirmed the optimum intumescence, coherent and strong barrier layer formation at an intermediate Zn^{2+} loading.

Keywords: Zinc chelate; Low density polyethylene; Fire retardant; Mannich condensation; Flammability

1. Introduction

Intumescent fire retardants (IFRs) are often phosphorus-nitrogen containing compounds, which are considered as promising candidates to substitute for the halogen-containing flame retardants, since there are no known environmental problems associated with their use[1-4]. The proposed mechanism of the IFR is based on swollen char acting as physical barrier, which slows down heat and mass transfer between the gas and the condensed phases[5]. However, an effective IFR loading is about 30 phr or more, which may be detrimental to the mechanical properties of the plastic, and make it more difficult to recycle. Therefore, attention was focused on how to improve the efficiency of the IFRs and so reduce their loading[6-8].

Recently, compounds containing metallic elements such as transition metal oxides and metal sulfates have been utilized for improving the flame retardancy of the IFR-polymer system[9-11]. These metal compounds can not only act in the vapor phase, but also in the condensed phase and at the gas/solid interface, so as to reduce the flammability through a chemical and/or physical mechanism[12-16].

Wu reported that zinc and nickel salts increased the limiting oxygen index (LOI) and decreased the heat release rate (HRR) in blends of polypropylene (PP)/ammonium polyphosphate (APP)/dipentaerythritol (DPER) [17]. Lewin reported that divalent and multivalent metal oxides could enhance the fire retardancy of intumescent systems based on APP and pentaerythritol (PER) in PP[18].

Although the metal compounds mentioned above can improve the fire retardancy of the IFR in a polymer, such blending of IFR and metal compounds can result in problems of heterogeneous distribution and incompatibility, reducing the fire retardant effectiveness. To avoid this, an IFR molecule with a metal ion in one molecule, zinc-tetraethyl (1,2-phenylenebis(azanediyl)) bis (2-hydroxylphenylmethylene) diphosphonate (Zn-TEPAPM) (Figure 1), was developed in our earlier work[9]. This is a metal chelate containing phosphorus, nitrogen and a metallic element. However, the fire retardancy of Zn-TEPAPM was not as good as expected[9]. When the content of Zn-TEPAPM was 25 wt% in low density polyethylene (LDPE), the reduction of peak

heat release rate (PHRR) of LDPE/Zn-TEPAPM was 41% and the char layer was not continuous, leaving a lot of holes in the residue from the cone calorimeter test. If the content of Zn-TEPAPM was 1 wt% and was blended with 19 wt% APP in LDPE, a more intact and continuous char layer was formed and the reduction of PHRR of LDPE/19APP/1Zn-TEPAPM reached 51%. The reason for such results is ascribed to the effect of different loadings of zinc ions on the fire retardancy of LDPE. However, due to the limitations of the structure of Zn-TEPAPM, it is difficult to change Zn^{2+} loading in TEPAPM.

Therefore, a novel oligomeric IFR chelate, zinc phosphonated poly(ethylene imine) (Zn-PEIP), containing phosphorus, nitrogen and zinc was designed and synthesized. As Fig. 1 shows, there are multiple coordination positions available on the branched chains of the oligomeric ligand to be chelated with metal ions. This allows the content of metal ions in the molecule to be varied from zero to a saturation value. By changing the zinc ion loading, the fire retardancy of such an oligomeric IFR chelate can be optimized and used to study the structure-property relationships.

The Mannich condensation was used to synthesize the phosphonated poly(ethylene imine) (PEIP), for use as an IFR ligand. Zinc (Zn) was chosen to be chelated with PEIP for its ability to improve the dehydrogenation during thermal degradation[19]. The chemical structure and thermal properties of Zn-PEIP and PEIP were characterized by infrared analysis (IR), NMR (including ^{13}C-NMR and ^{31}P-NMR) and thermogravimetric analysis (TGA). With the varied content of Zn in Zn-PEIP, the effects of Zn-PEIP in low density polyethylene (LDPE) were studied with respect to thermal stabilization, burning behaviour and flame retardancy, using TGA, LOI, the cone calorimeter (CONE), scanning electron microscope (SEM) and X-ray diffraction (XRD).

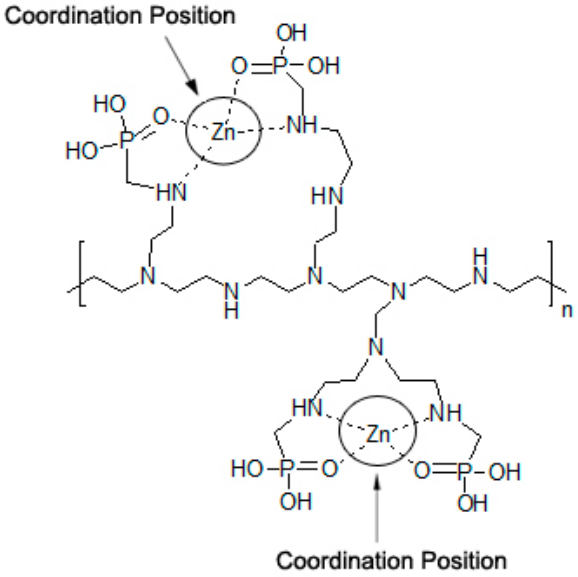

Fig. 1 Proposed structure of Zn-PEIP

2. Experimental

2.1 Materials

LDPE (2102TN26) with a melt flow index of 2.1–2.9 g/10min and a density of 0.920–0.922 g/m^3 was purchased from Sinopec Qilu Company Ltd. (Zibo, China). LDPE grafted with about 1.0 wt% maleic anhydride (TRD-100L, LDPE-g-MA) was provided by Wujiang Siruida Plastic Industry Co., Ltd. (Wujiang, China). Poly(ethylene imine) (PEI, M_w = 10 000, 99 wt%) was purchased from Aladdin-reagent Co., Ltd. (Shanghai, China). Phosphonic acid ($HPO(OH)_2$), concentrated hydrochloric acid solution (HCl), formaldehyde solution (CH_2O) of 37 wt%, diethanolamine and anhydrous ethanol (C_2H_5OH) were purchased from Sinopharm Chemical Reagent Co. Ltd. (Shanghai, China). Sodium hydroxide (NaOH) was purchased from Xilong Chemical Reagent Co. Ltd. (Guangzhou, China). Zinc acetate ($Zn(OOCCH_3)_2{\cdot}2H_2O$, Znac) was purchased from the Yixing 2nd Chemical Reagent Factory (Yixing, China). All chemical reagents were used without further purification.

2.2 The synthesis of PEIP and Zn-PEIP

2.2.1 The synthesis of PEIP

PEIP was obtained using the Mannich condensation reaction of poly(ethylene imine) (PEI), formaldehyde and phosphonic acid. 16.4 g of phosphonic acid and 10 g of PEI were dissolved in 100 mL of HCl in a 250 mL three-neck flask equipped with a mechanical stirring and reflux condenser. When the above solution was heated to reflux, 32 mL of 37 wt% formaldehyde solution was added dropwise into the flask over a period of 1 h. Then, the system was heated under reflux for 1 h. When cooled to room temperature, the mixture was neutralized by diethanolamine and the crude PEIP product precipitated. This was filtered and washed three times using anhydrous ethanol. Finally, the PEIP product was dried under vacuum as a yellow powder with a yield of 95%. The synthesis route is illustrated in Fig. 2(a).

2.2.2 The synthesis of Zn-PEIP

A three-neck flask was charged with different amounts of Znac, 15 g of PEIP, 2 g of NaOH and 500 mL of anhydrous ethanol. The mixture was stirred under nitrogen for 7 h under reflux. After cooling to room temperature, the yellow suspension was filtered and washed thoroughly with anhydrous ethanol, and then dried at 50 °C under vacuum to a constant weight. In order to prepare the Zn-PEIP with different Zn^{2+} loadings, the amount of Znac was varied from 0.1 mol, 0.07 mol, 0.05 mol, 0.03 mol, 0.01 mol, 0.007 mol down to 0.003 mol. The corresponding Zn chelates are named as Zn-PEIP-0.1, Zn-PEIP-0.07, Zn-PEIP-0.05, Zn-PEIP-0.03, Zn-PEIP-0.01, Zn-PEIP-0.007 and Zn-PEIP-0.003. The chelation step in the synthesis route is illustrated in Fig. 2(b).

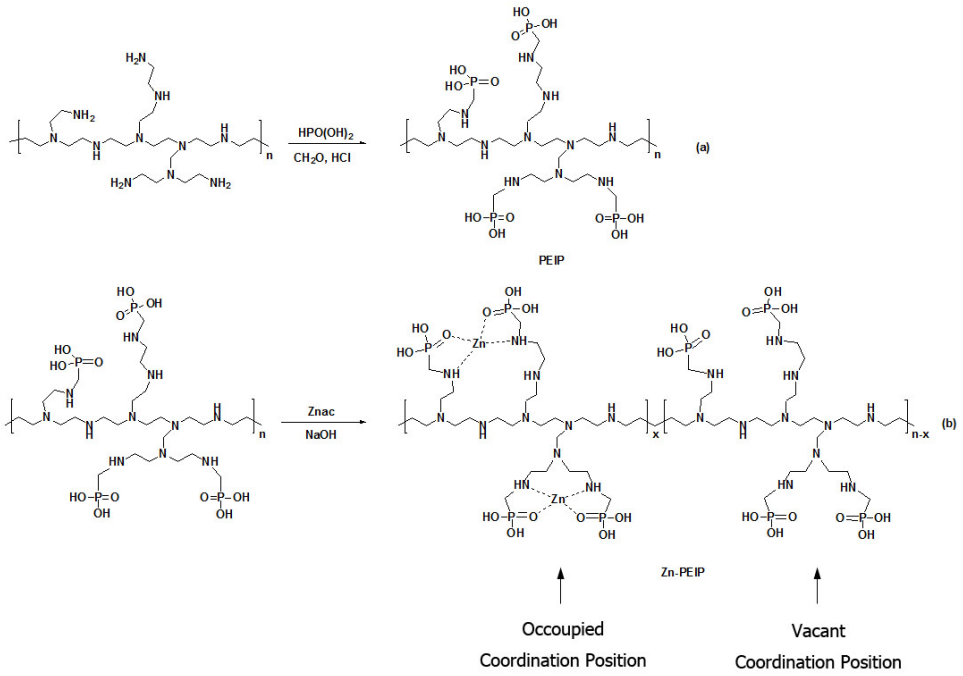

Fig. 2 The synthesis route of PEIP (a) and Zn-PEIP (b)

2.3 Preparation of fire retardant LDPE composites

The LDPE composites were prepared via melt compounding at 160 °C in Thermo-Haake rheomixer with a rotor speed of 60 rpm, according to the formulations presented in Table 1. The prepared materials were transferred into a mold and preheated for 5 min at 120 °C, and then pressed at 15 MPa for 8 min, followed by pressing at room temperature under the same pressure for 5 min.

Table 1 The formulation of flame retardant LDPE with Zn-PEIP and PEIP

Sample ID	LDPE /wt%	LDPE-g-MA /wt%	PEIP /wt%	Zn-PEIP /wt%
LDPE	95	5		
LDPE/Zn-PEIP-0.1	70	5		25
LDPE/Zn-PEIP-0.07	70	5		25
LDPE/Zn-PEIP-0.05	70	5		25
LDPE/Zn-PEIP-0.03	70	5		25
LDPE/Zn-PEIP-0.01	70	5		25
LDPE/Zn-PEIP-0.007	70	5		25
LDPE/Zn-PEIP-0.003	70	5		25
LDPE/PEIP	70	5	25	

2.4 Characterization

Infrared spectra (IR) were recorded on a Nicolet Nexus-470 FTIR spectrometer as KBr disks. ^{13}C solid NMR and ^{31}P solid NMR spectra were recorded on a DSX 300 spectrometer (300 MHz, Bruker). TG analysis was performed on a TG 209F1 thermal analyzer at a heating rate of 20 °C·min^{-1} in N_2 and air (Netzsch), respectively, from room temperature to 650 °C. Limiting oxygen index (LOI) values were determined using an HC-2 Oxygen Index instrument on sample strips of dimensions of 120 × 6 × 3 mm^3 according to ASTM D2863 (Jiang Ning Analytical Instrument Co Ltd). The combustion parameters were measured according to ISO 5660 using a cone calorimeter (Govmark) at a heat flux of 50 kW·m^{-2}. The dimensions of all samples for the cone calorimeter measurements are 100 × 100 × 3 mm^3. Morphology of the residual chars collected after the cone calorimeter tests was obtained using a S3400N field emission scanning electron microscope (Hitachi). The phase and crystallographic structures of the samples were examined by XRD on a Rigaku D/MAX 2550/PC X-ray diffractometer working with CuKα radiation.

3. Results and discussion

3.1. Characterization of Zn-PEIP and PEIP

Since the only difference between the Zn-PEIP samples was the variable amount of Zn^{2+} in the molecular structure, the structure and thermal properties of Zn-PEIP with the highest zinc loading (Zn-PEIP-0.1) were assumed to be representative of all Zn-PEIPs. Fig. 3 shows the FTIR spectra of PEIP and Zn-PEIP-0.1. PEIP shows peaks around 1167 cm^{-1}, attributed to uncoordinated P=O groups, which are more abundant than in Zn-PEIP-0.1. This is due to the reduction in bond strength of the P=O groups coordinated to Zn^{2+} in Zn-PEIP-0.1, shifting absorption below 1167 cm^{-1}. At the same time, the absorption of P-O group at 1066 cm^{-1} does not appear to change, which indicates that coordination does not occur between P-OH and Zn^{2+}, only between P=O and Zn^{2+}. This statement is underpinned by the change of absorption

peak of NH_2^+. Because of the presence of PO_3H groups in PEIP, nitrogen atoms in PEIP can be protonated by P-OH groups[20], forming NH_2^+ groups. These are expected to give two bands around 3000 and 2700 cm^{-1}, which are usually broad, unresolved and extended to around 2200 cm^{-1}.[20] Indeed, the IR spectrum of PEIP in Fig. 3 shows a broad and shallow band at 2000–2500 cm^{-1}, revealing the presence of the protonated amine in PEIP. After chelation, the NH_2^+ bands become weaker. Moreover, the absorption peak at 1467 cm^{-1}, ascribed to bending of the NH_2^+ groups, is also weakened, resulting from the coordination bonds formed between P=O, N-H and Zn^{2+}. As Fig. 1 and Fig. 2 show, chelation between P=O, Zn^{2+} and N-H groups can form two five-membered rings, resulting in a more stable chelate structure compared to chelates of just P-OH groups and Zn^{2+}.

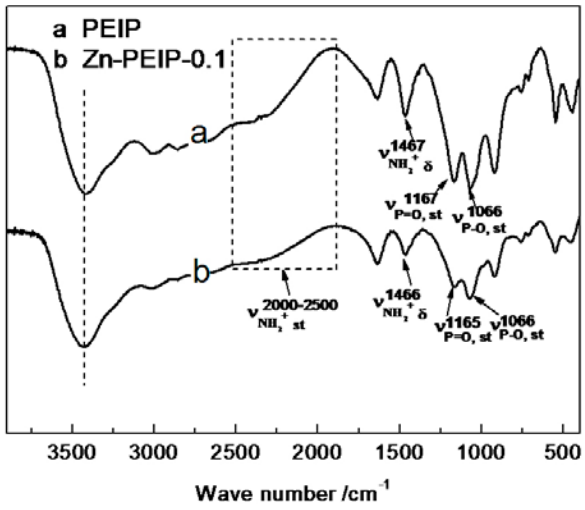

Fig. 3 IR spectra of PEIP and Zn-PEIP-0.1

The structures of PEIP and Zn-PEIP-0.1 were further characterized by solid-state ^{13}C-NMR and ^{31}P-NMR spectra as Fig. 4 (a) and (b) shows, respectively. In Fig. 4(a), there is only one obvious broad peak at 51.5 ppm in the ^{13}C-NMR spectrum of PEIP. This is because the chemical shifts of the carbons in C-C, C-P and C-N groups are similar in the PEIP, and their peaks overlap each other. After chelation, the broad peak of Zn-PEIP-0.1, shown in Fig. 4(a), shifted slightly to 51.3 ppm. This might be the result of the π-backbonding effects formed by the chelation of Zn and the PEIP ligand. ^{31}P-NMR spectra in Fig. 4(b) also indicate the difference of the structures of PEIP and Zn-PEIP-0.1. As described earlier, both NH and NH_2^+ groups exist in PEIP. That is to

say, the PO_3H groups may exist as it is or a PO_3^- ion, after protonation of the amine group to NH_2^+. This results in two phosphorus absorption peaks of PEIP in Fig. 4(b). Since ionization shifts P to a lower field, absorbance at 7.8 ppm is attributed to PO_3H and the smaller peak at 20.9 ppm is ascribed to PO_3^- ion. After the chelation with Zn, the ^{31}P NMR spectrum of Zn-PEIP-0.1 shows two strong absorption peaks. The unchelated PO_3H peak as before shows that not all chelation sites contained zinc, while the peak at 18.3 ppm can be assigned to P in the chelate of P=O, Zn^{2+} and N-H groups, since the π-backbonding effects are formed by the chelation of Zn and the PEIP ligand.

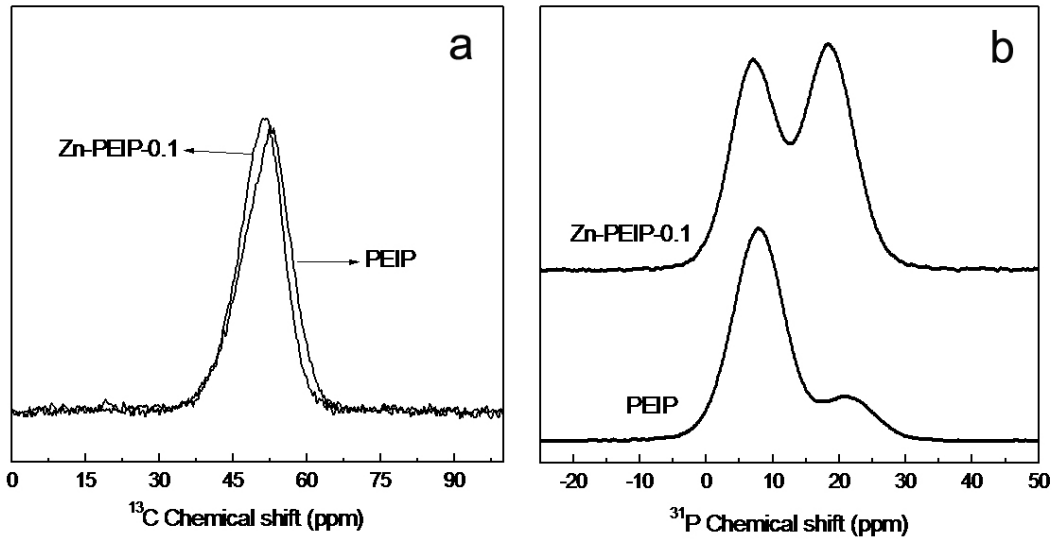

Fig. 4 ^{13}C-NMR (a) and ^{31}P-NMR (b) spectra of PEIP and Zn-PEIP-0.1

Since the zinc (II) ion may affect the thermal stability of the chelate, Zn-PEIPs with different amounts of zinc were characterized by TGA in nitrogen. Fig. 5 shows the TGA and DTG thermograms of the Zn-PEIPs. The detailed data, including the onset temperature of decomposition (T_{onset}), maximum decomposition temperature (T_{max}) and residue percentage at 650 °C, are summarized in Table 2.

As Fig. 5 and Table 2 show, the initial decomposition temperatures (T_{onset}) of Zn-PEIPs decrease from 228 °C to 191 °C as the amount of Zn^{2+} ions is reduced. As PEIP had the lowest T_{onset} of 179 °C, it implies that chelation between PEIP and Zn^{2+} increases the thermal stability of Zn-PEIPs. The residue at 650 °C follows the same trend as T_{onset} of Zn-PEIPs. Zn-PEIP-0.1 has the highest amount of residue at 650 °C

of 59.5 wt%. If residue was composed of $Zn(PO_3)_2$, the residue amount would be 45%, which suggests a significant proportion of the PEIP ligand contributed to the amount of residue as a char. PEIP has the smallest residue with only 26.5 wt%, indicating the role of Zn^{2+} in the char forming process. According to Petersen[21], divalent ions such as zinc (II) are known to promote crosslinking and dehydration reactions. During the thermal degradation of Zn-PEIPs, Zn^{2+} may catalyze the dehydration of the PEIP ligand and polyphosphoric acid will be formed. Then, Zn^{2+} reacts with polyphosphoric acid to form a crosslinked network through salt bridges, leading to increased residue formation. Hence, the more Zn^{2+} in Zn-PEIPs, the more residue will be formed. Similar results were also found by Chen[22] and Song[23]. They observed that nickel, zinc and chromium ions could increase the char formation in PP with an intumescent fire retardant, and they attributed this behavior to the reaction between the metal ions and the polyphosphoric acid through salt bridges.

Fig. 5b shows that Zn-PEIPs underwent multi-step thermal degradation processes. Zn-PEIP-0.1, Zn-PEIP-0.07 and Zn-PEIP-0.05 have two main weight-loss stages which can be assigned to the dehydration of PEIP and char formation. With the decrease of the chelation of Zn^{2+}, four weight-loss stages are observed. The residue formed at about 350 ^{o}C may be unstable because there is less Zn^{2+}, hence less crosslinking. It may continue to decompose at higher temperatures until a more stable residue forms. The less Zn^{2+} in Zn-PEIPs, the closer the thermal stability of Zn-PEIPs is to that of PEIP. Without Zn^{2+}, dehydration of PEIP still occurs, but the degree of crosslinking may not be the same as that of the Zn-PEIPs. Therefore, the least residue is formed by PEIP.

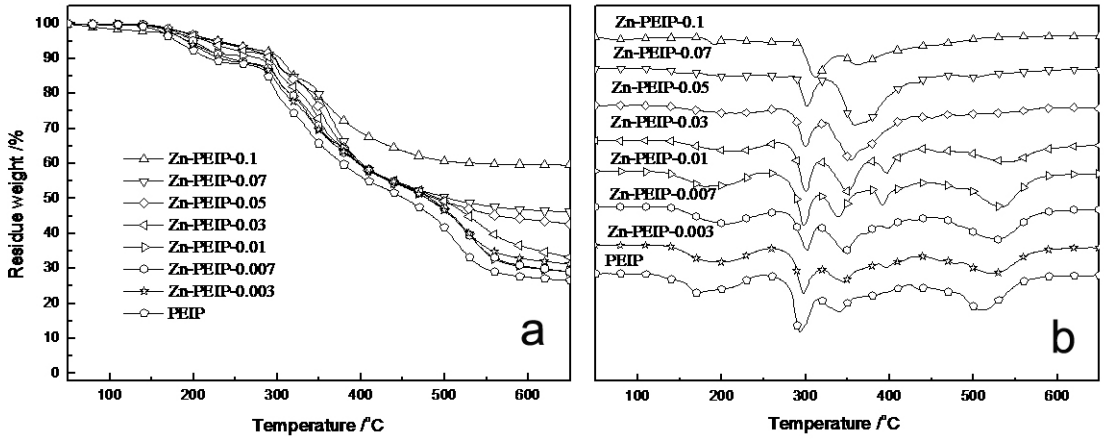

Fig. 5 TG (a) and DTG (b) curves of PEIP and Zn-PEIPs in N_2

Table 2 TGA data of PEIP and Zn-PEIPs in N_2

Sample	T_{onset} /°C [a]	T_{max} /°C [b]	Residue at 650°C /wt %
Zn-PEIP-0.1	228	312, 361	59.5
Zn-PEIP-0.07	228	302, 358	46.2
Zn-PEIP-0.05	226	300, 354	42.8
Zn-PEIP-0.03	215	300, 350, 396, 541	33.2
Zn-PEIP-0.01	193	298, 338, 391,534	29.1
Zn-PEIP-0.007	199	301, 346, 529	29.1
Zn-PEIP-0.003	191	297, 344, 520	31.3
PEIP	179	293, 340, 509	26.5

a: designated as the onset point at 5wt % weight loss, b: maximum decomposition temperature

3.2. Properties of the LDPE/Zn-PEIP and LDPE/PEIP blends

3.2.1 Thermal stability

After ignition, all the oxygen at the polymer-flame interface is consumed. This means that the thermal decomposition in an inert atmosphere is the appropriate condition for determining the fuel production rate of a flaming material [24, 25]. The thermal decomposition of LDPE and LDPE blended with PEIP and Zn-PEIPs in N_2 shown in Fig. 6, best represents the fuel release. The detailed data are summarized in Table 3.

For LDPE, the degradation begins at 391 °C in N_2 and the maximum weight loss rate appears at 469 °C, with 0 wt % residue at 650 °C. Addition of PEIP and Zn-PEIPs results in an increase of T_{max} by 11-14 °C, showing a small improvement in the thermal stability of LDPE. As described above, the crosslinks formed by Zn-PEIPs

will lead to the formation of the protective network and enhanced charring, increasing the LDPE degradation temperature. T_{onset} and the weight of residue at 650 °C decrease with the decrease of Zn^{2+} in Zn-PEIPs, corresponding to that of Zn-PEIPs in N_2. As expected, the lowest T_{onset} of 298 °C and the residue at 650 °C of 6.94 wt % is that of LDPE/PEIP without any Zn^{2+}.

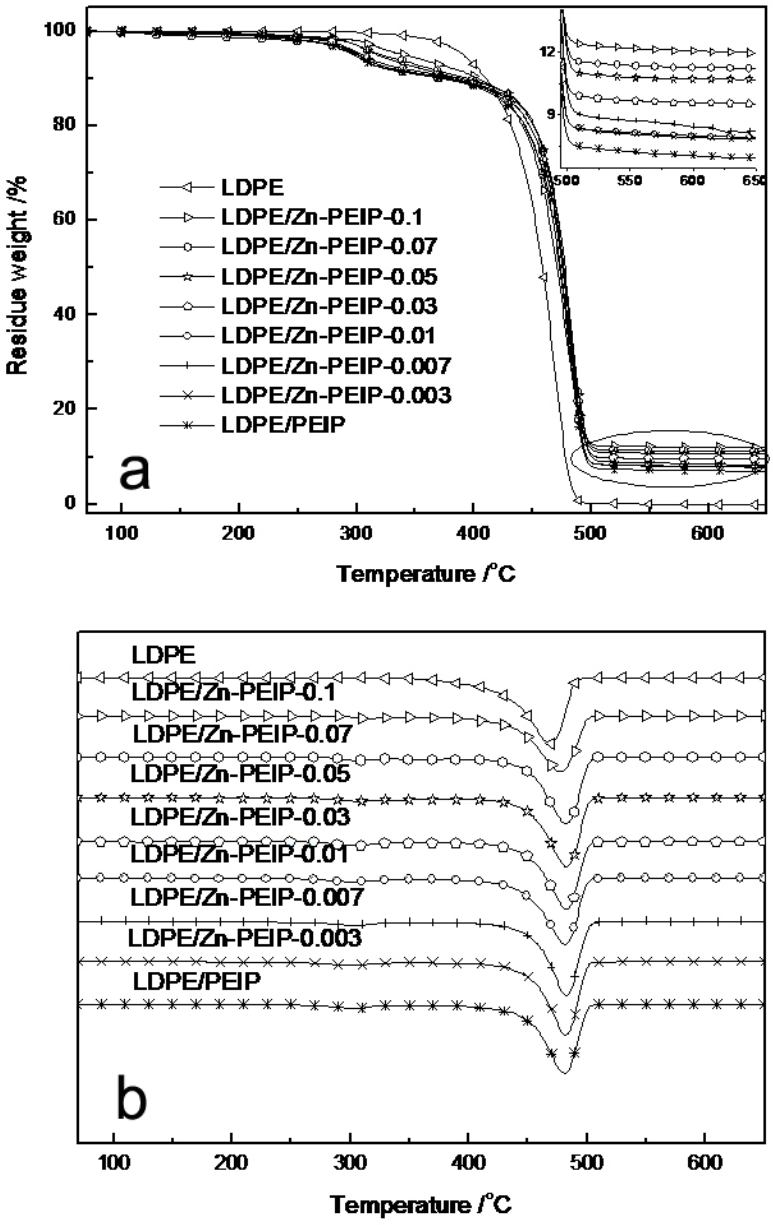

Fig. 6 TG (a) and DTG (b) curves of LDPE, LDPE/PEIP and LDPE/Zn-PEIPs in N_2

Table 3 TGA data of LDPE, LDPE/PEIP and LDPE/Zn-PEIPs in N_2

Sample	T_{onset} /°C [a]	T_{max} /°C [b]	Residue at 650°C /%
LDPE	391	469	0
LDPE/Zn-PEIP-0.1	387	480	13.88
LDPE/Zn-PEIP-0.07	330	483	11.01
LDPE/Zn-PEIP-0.05	317	480	10.34
LDPE/Zn-PEIP-0.03	311	481	8.28
LDPE/Zn-PEIP-0.01	312	482	9.01
LDPE/Zn-PEIP-0.007	308	482	8.49
LDPE/Zn-PEIP-0.003	308	482	7.39
LDPE/PEIP	298	480	6.94

a: designated as the onset point at 5 wt % weight loss, b: maximum decomposition temperature

3.2.2 Flammability

Limiting oxygen index test (LOI) was conducted to investigate the flammability of the materials. It determines the minimum oxygen concentration in a mixture of oxygen and nitrogen required to support downward flame spread along the sample strip[26]. The results of LOI tests for LDPE and its composites are shown in Table 4. The LOI of LDPE is 17.9 indicating its inherent flammability. The addition of PEIP increased the LOI to 20.4, rising to 24.1 for LDPE/Zn-PEIP-0.01. Further increase of Zn^{2+} in Zn-PEIPs decreases the LOI. The increase in LOI is in contrast to the higher residue yield found by TGA.

Table 4 Results from LOI measurements

Sample	LOI
LDPE	17.9
LDPE/Zn-PEIP-0.1	20.6
LDPE/Zn-PEIP-0.07	21.9
LDPE/Zn-PEIP-0.05	23.2
LDPE/Zn-PEIP-0.03	23.5
LDPE/Zn-PEIP-0.01	24.1
LDPE/Zn-PEIP-0.007	23.5
LDPE/Zn-PEIP-0.003	22.3
LDPE/PEIP	20.4

Cone calorimetry is used for investigating the burning behavior of polymeric materials, which can provide various parameters such as time to ignition (t_{ign}), peak heat release rate (PHRR), total heat release (THR) and average specific extinction

area (ASEA) [27,28]. Fig. 8 and Table 5 show the cone calorimetric data for LDPE, LDPE/Zn-PEIPs and LDPE/PEIP blends, respectively. These show very significant reduction in flammability for all the PEIP and Zn-PEIP materials tested.

Fig. 7 shows that LDPE burns very rapidly after ignition and a large PHRR of 1645 $kW \cdot m^{-2}$ appears at around 135s. In the case of LDPE/PEIP systems, PHRR and THR values are reduced by 86.3 % and 30.2 % with the addition of PEIP, demonstrating PEIP alone slows down the combustion process. Adding Zn-PEIPs to LDPE, the THR values decreased to an even greater extent. As shown in Table 5, the THR values for LDPE/Zn-PEIP-0.1, LDPE/Zn-PEIP-0.05 and LDPE/Zn-PEIP-0.01 are 57, 55 and 51 $MJ \cdot m^{-2}$, lower than that of the LDPE/PEIP blend (74 $MJ \cdot m^{-2}$). The values of THR decrease with the decrease of the content of Zn^{2+}, but increase when Zn^{2+} is absent from the LDPE/PEIP system. The fire behavior of LDPE in the cone calorimeter was in agreement with the result from the LOI measurement. Although LDPE/Zn-PEIP-0.01 has the highest PHRR values of the zinc containing materials, this occurred later, so had a lesser effect on the fire growth properties.

Moreover, there are notable differences in the t_{ign}s of LDPE/Zn-PEIPs and LDPE/PEIP. The t_{ign} of LDPE is 55 s, and that for LDPE/Zn-PEIP-0.1 is prolonged to 64 s. With the decrease of Zn^{2+} in LDPE/Zn-PEIPs systems, the t_{ign} increase progressively. The t_{ign} of LDPE/Zn-PEIP-0.01 and LDPE/PEIP are 160s and 153s, respectively, which is much longer than that of LDPE or LDPE/Zn-PEIP-0.1 or 0.05.

According to the analysis described above, the LOI and Cone calorimetry results support each other, while TGA results of the blend are different. That is because the amounts of 5-8 mg of sample in TGA tests are so small that they cannot form an effective insulating barrier to prevent heat and fuel transfer. Although the increase of Zn^{2+} led to the higher residue yield found by TGA, the increased amount of char formation is not the only factor to get better flame retardancy. The swelling degree and the mechanical property of char layer are also very important factors. In order to illustrate the effect of zinc loading on flame retardant properties, a schematic char formation process is shown in Fig. 8.

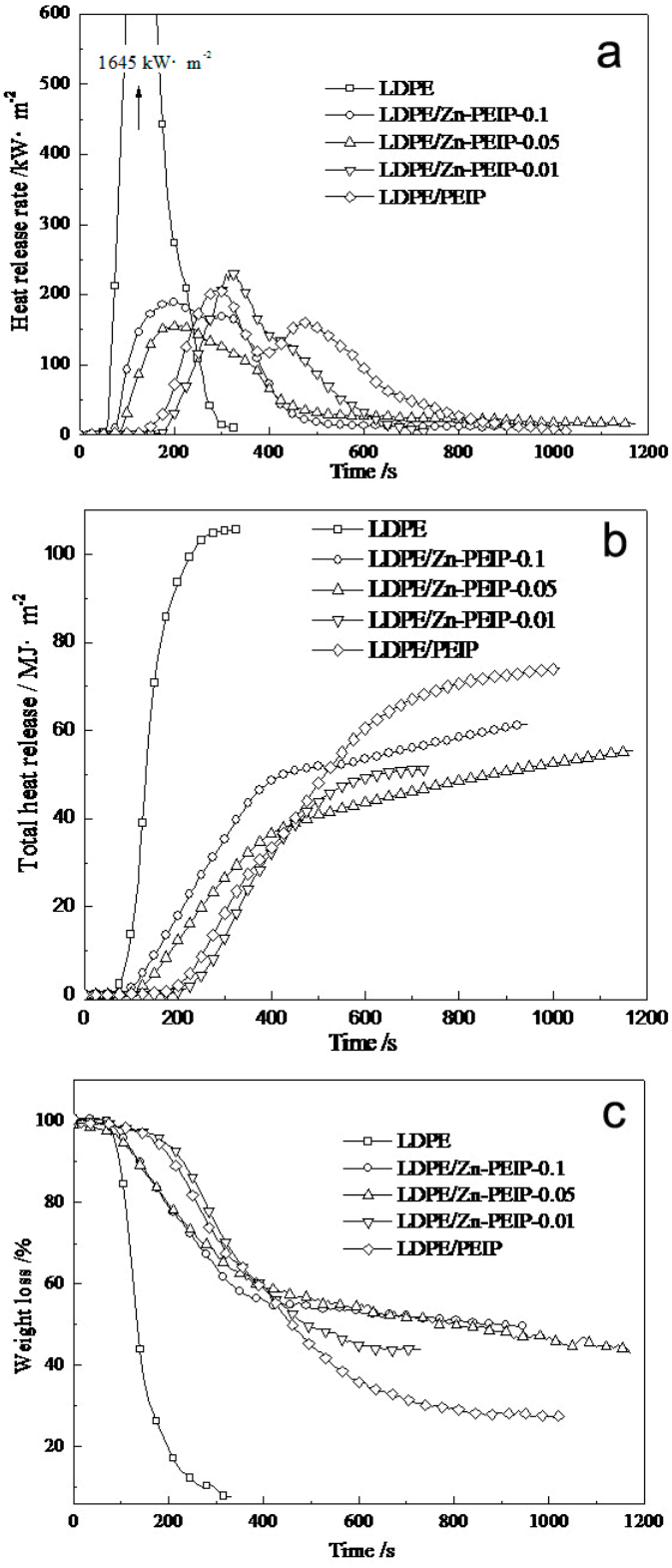

Fig. 7 (a) Heat release rate curves, (b) total heat release curves, and (c) mass loss curves of LDPE, LDPE/PEIP and LDPE/Zn-PEIPs in the cone calorimeter test

Table 5 Combustion parameters obtained from burning in the cone calorimeter test

Samples	t_{ign} / s	PHRR /kW·m^{-2}	THR /MJ·m^{-2}	ASEA /m^2·kg^{-1}	CO yield /kg·kg^{-1}	Residue /wt %
LDPE	55	1645	106	431	0.0557	6.27
LDPE/Zn-PEIP-0.1	64	190	57	630	0.0554	50.37
LDPE/Zn-PEIP-0.05	74	156	55	703	0.0673	43.63
LDPE/Zn-PEIP-0.01	160	234	51	730	0.0706	43.97
LDPE/PEIP	153	226	74	877	0.0730	27.05

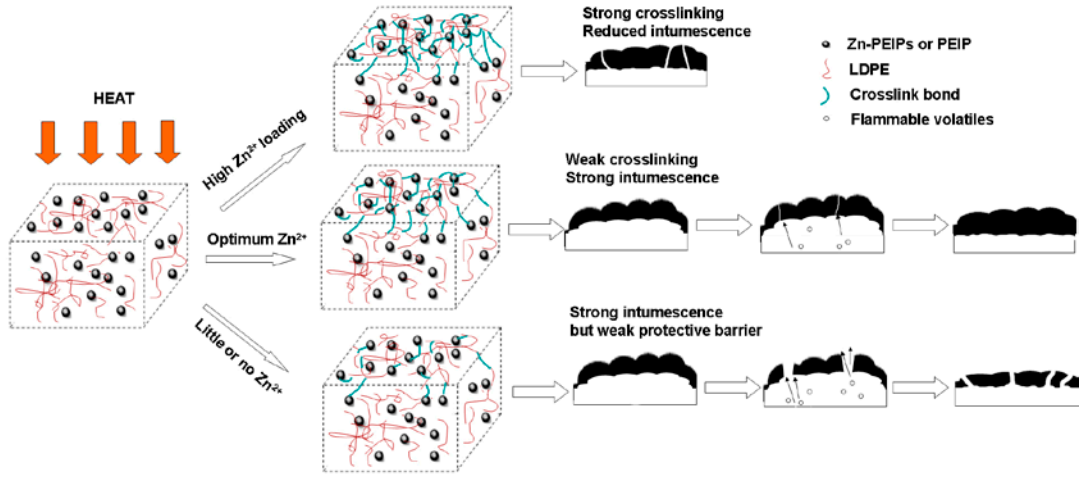

Fig. 8 Schematic of char formation process of Zn-PEIPs and PEIP in LDPE

It is generally accepted that, when heated in an atmosphere containing oxygen, LDPE chains may undergo autoxidation, with the formation of hydroperoxides and then hydroxyl groups on the main chain[29]. These hydroxyl groups can be phosphorylated by the degradation product of PEIP through dehydration. With the catalytic effect of Zn^{2+}, further dehydration occurs on LDPE. The formation of salt bridges between Zn^{2+} and these phosphate groups may enhance crosslinking. At the same time, according to the TG analysis of Zn-PEIPs, the flame retardant Zn-PEIPs can also form a crosslinked network by the catalysis of Zn^{2+} during combustion. Both types of crosslinks described above are important factors to the char-formation processes, and further affect the mechanical performance of the char layer. Song found that a certain amount of metal ions and polyphosphoric acid can form a crosslinked network, through salt bridges, to form a more compact residual layer with better mechanical performance[23]. Thus, the char-formation processes and the quality of the protective char layer of LDPE/Zn-PEIPs blends are affected significantly by the Zn^{2+} loading.

As shown in Fig. 8, when the content of Zn^{2+} in the fire retardant LDPE system is too high, a network with high crosslink density is formed, resulting in an increase in melt viscosity of the LDPE composite. A more rigid residue was obtained at high Zn^{2+} loading. As shown in Table 5, the 50.37 wt% residue of LDPE/Zn-PEIP-0.1 is much higher than that in TGA test, demonstrating the formation of a protective barrier layer, a physical, rather than chemical fire retardant effect. PHRR and THR values of LDPE/Zn-PEIP-0.1 are also greatly decreased.

However, such a strong network may also prevent the significant swelling associated with IFRs. Due to the high melt viscosity and inflexible network, the crosslinked polymer may instead release gases through defects in its structure, such as holes or cracks, which then allow the release of flammable volatiles. The transfer of heat from the flame to the underlying substrate and the evolution of fuel from it led to the sustained combustion of LDPE. Higher THR and lower LOI values were obtained from LDPE/Zn-PEIP-0.1 than from other LDPE/Zn-PEIP systems with less Zn^{2+}.

For the LDPE/Zn-PEIP-0.05 blend, the decrease of Zn^{2+} may also lower the crosslink density in the matrix. The char layer becomes more flexible and protects the underlying matrix more efficiently than that formed in the LDPE/Zn-PEIP-0.1, as shown by the higher LOI value, the prolonged $t_{ign,}$ and the lowest value of PHRR shown in Table 4 and Table 5. Due to the relatively high loading of Zn^{2+} in the LDPE/Zn-PEIP-0.05 blend, the THR value is not the lowest of the LDPE/Zn-PEIP systems and the flexibility of the char layer needs to be improved through further decrease of Zn^{2+}.

With the further decrease of Zn^{2+} in the LDPE/Zn-PEIP-0.01, the density of network reaches an optimum value. The protective barrier layer is greatly improved with sufficient flexibility. The lowered melt viscosity of LDPE/Zn-PEIP-0.01 and the further dehydration results in a more coherent char layer being built up, which results in the highest LOI values and lowest THR value. The delay in the major peak and a slight shoulder peak on the HRR curve of LDPE/Zn-PEIP-0.01 suggest changes to the stages of char formation in the cone calorimeter.

In the LDPE/PEIP system, the LDPE chains can still be phosphorylated and form a

network through dehydration. Without catalysis of Zn^{2+}, the crosslink density is lower than that of LDPE/Zn-PEIPs, but the more flexible char swells better. The t_{ign} of 153s of LDPE/PEIP indicates that the intumescent char is effective in protecting the polymer from being ignited. However, with the continuous attack of heat, the char layer cracks. These cracks form pathways for the escape of flammable volatiles reducing the fire retardancy. Therefore, the THR values of for LDPE/PEIP increased to 74 $MJ \cdot m^{-2}$ compared with LDPE/Zn-PEIP-0.01, and the LOI value also decreased to the lowest value compared with the LDPE/Zn-PEIPs.

The progressive decrease of THR from LDPE/Zn-PEIP-0.1 to 0.01, while the residual mass also decreases, suggests some gas phase inhibition may also be occurring. This is supported by the significant increase in ASEA shown in Table 5. For LDPE/PEIP, the value of ASEA increases from 431 $m^2 \cdot kg^{-1}$ (for LDPE) to 877 $m^2 \cdot kg^{-1}$. Under the protection of the defective char layer formed by PEIP, the underlying polymer undergoes decomposition and incomplete combustion, increasing the emission of smoke. However, when the Zn^{2+} loading increases, the ASEA decreases gradually from 877 $m^2 \cdot kg^{-1}$ to 630 $m^2 \cdot kg^{-1}$, indicating that Zn^{2+} suppresses the production of smoke. The yield of CO also follows the same trend. Such results are consistent with our previous study[9].

3.2.3 Analysis of the char residue

The optical and SEM photos of the residues after the cone calorimeter test are shown in Fig. 9 and 10, which are consistent with the hypothesis illustrated in Fig. 8. As expected, with the decrease of Zn^{2+} in LDPE/Zn-PEIPs system, the char layer formed in the cone calorimetric tests began to swell and become more continuous and intumescent.

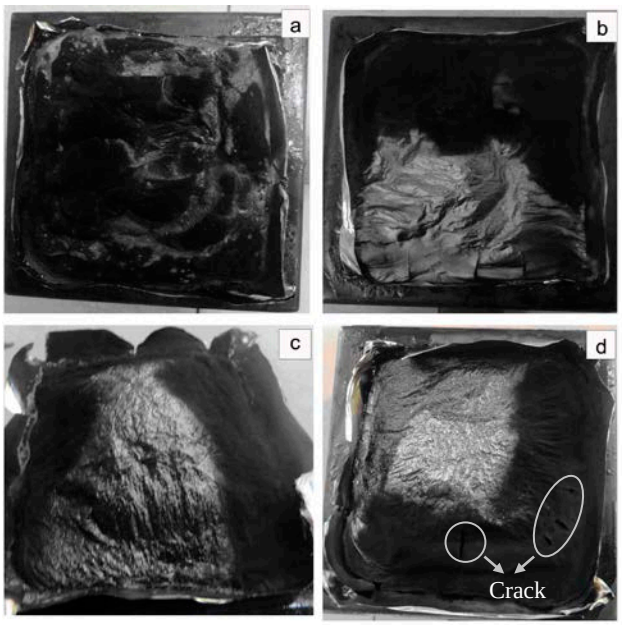

Fig. 9 Optical images of residues after the cone calorimeter test for (a) LDPE/Zn-PEIP-0.1, (b) LDPE/Zn-PEIP-0.05, (c) LDPE/Zn-PEIP-0.01 and (d) LDPE/ PEIP

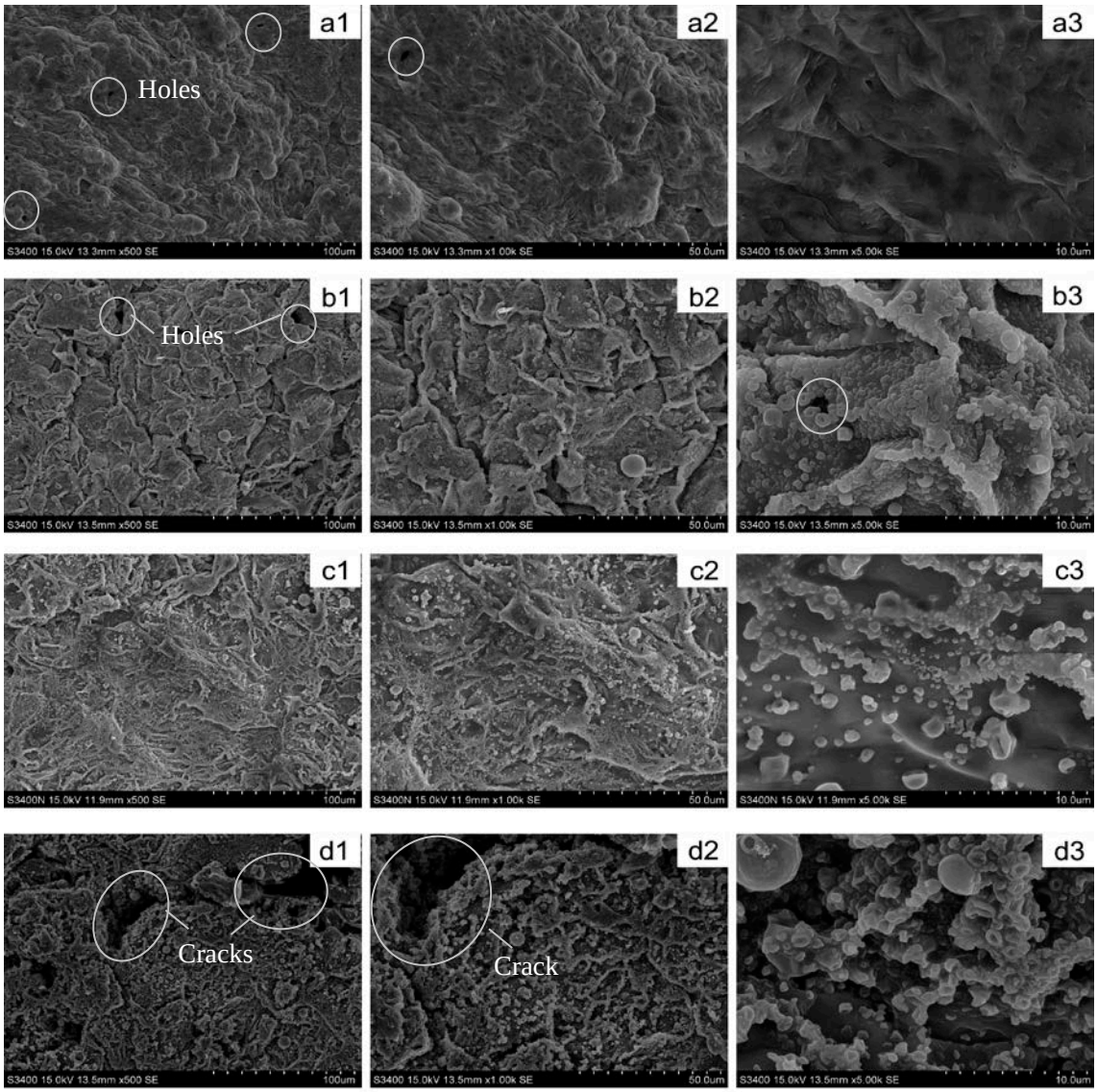

Fig. 10 SEM images of the char residues for LDPE/Zn-PEIP-0.1 (a1: ×500, a2: ×1k, a3 ×5k magnification); LDPE/Zn-PEIP-0.05 (b1: ×500, b2: ×1k, b3: ×5k magnification); LDPE/Zn-PEIP-0.01 (c1: ×500, c2: ×1k, c3: ×5k magnification); LDPE/PEIP (d1: ×500, d2: ×1k, d3: ×5k magnification) after the cone calorimeter test

Fig. 9(a) shows, a thick and compact char layer was formed by the LDPE/Zn-PEIP-0.1 sample. The surface morphology of the char is more like a frozen liquid with high viscosity. From the images of the surface in Fig. 10(a-1, a-2 and a-3), the chars are dense with a few holes and less obvious bubbles on the surface, because of the poor flexibility of char formed in LDPE/Zn-PEIP-0.1 system. For the LDPE/Zn-PEIP-0.5 sample, a little intumescent char layer can be seen from Fig. 9(b)

while holes are observed in Fig. 10(b-1, b-2 and b-3).

Fig. 9 (c) shows better intumescence in the LDPE/Zn-PEIP-0.01 system. Especially in Fig. 10(c-3) at high magnification, the surface of the char layer is smooth and intact with swollen bubbles, which act as a more effective thermal barrier to reduce heat transfer from the flame to the underlying substrates, and thus reduce the total heat release rate of LDPE. Although a typical intumescent morphology is shown in Fig. 9 (d) and Fig. 10 (d-1, d-2 and d-3) for the LDPE/PEIP system, there are apparent cracks appearing on the surface of the char.

The XRD patterns of the residue of LDPE/Zn-PEIPs and LDPE/PEIP after the cone calorimeter test are given in Fig. 11. For LDPE/Zn-PEIP-0.1, the residue clearly has a significant degree of crystallinity. The peaks in the diffractogram located at 19.5°, 21.6°, 23.1°, 25.6°, 27.1° and 31.8° could resulted from zinc phosphate, $Zn(PO_3)_2$. This suggests that Zn^{2+} reacts with polyphosphoric acid (decomposition products of PEIP) to form the crosslinked network. Through further dehydration, $Zn(PO_3)_2$ was finally formed in the residue. The XRD spectrum of LDPE/Zn-PEIP-0.05 is quite different from that of Zn-PEIP-0.1. The amorphous proportion increased, indicating a different degradation pathway of LDPE/Zn-PEIP-0.05. The peaks at 12.6°, 21.7°, 28.2° and 32.6° are attributed to $ZnH_2P_2O_7$, corresponding to degradation products with less dehydration because of the decrease of Zn^{2+}. With further decrease of Zn^{2+}, the XRD spectra of LDPE/Zn-PEIP-0.01 and LDPE/PEIP residue appear completely amorphous.

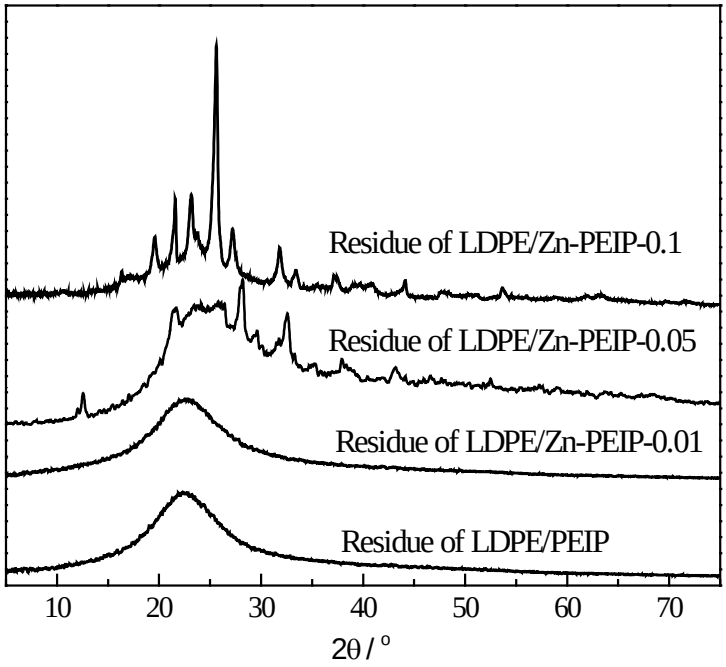

Fig. 11 XRD spectra of residues for LDPE/Zn-PEIPs and LDPE/PEIP after the cone calorimeter test

FTIR spectra of the intumescent residual for LDPE/Zn-PEIPs and LDPE/PEIP after the cone calorimeter test are shown in Fig. 12. The four residues have several peaks in common. The peak around 1630 cm^{-1} is assigned to stretching of phenyl, indicating the formation of polyaromatic carbonaceous species during combustion[23]. The broad peak at 997–1031 cm^{-1} is attributed to stretching of P-O in P-O-C and P-O-P[7, 30]. The peak of LDPE/Zn-PEIP-0.1 observed at 1230 cm^{-1} corresponds to stretching of P=O. With the decrease of Zn^{2+}, this becomes broader over the range 1170-1240 cm^{-1}. The IR spectra demonstrate that Zn-PEIPs and PEIP can produce phosphoric and polyphosphoric acids during combustion, which promote dehydration forming a carbonaceous char.

The new peaks around 1400 cm^{-1} and the new broad peaks of 2900-3120 cm^{-1} in the IR spectra of LDPE/Zn-PEIP-0.05, LDPE/Zn-PEIP-0.01 and LDPE/PEIP may be attributed to the C-H vibration of aliphatic groups[10]. Although more flammable, these will improve the flexibility, allowing greater intumescence and better protection with the decreasing content of Zn^{2+} in flame retarded LDPE.

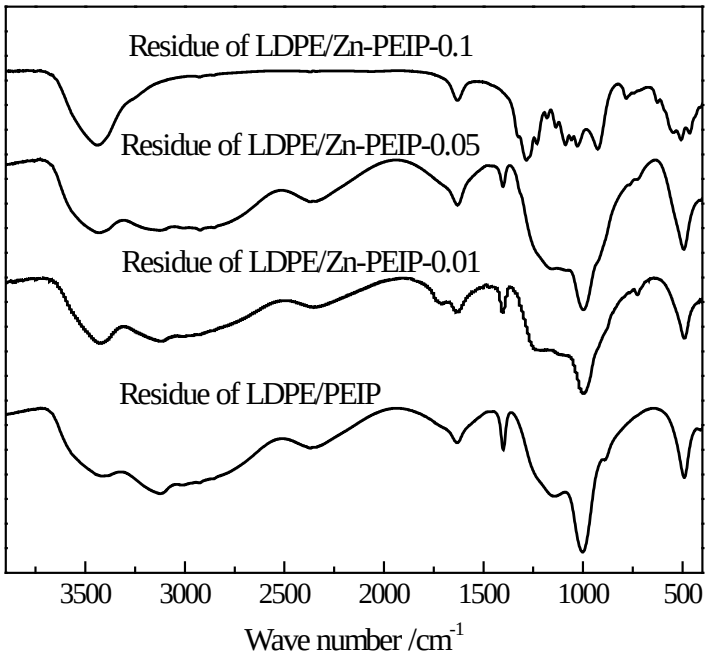

Fig. 12 IR spectra of char residues for LDPE/Zn-PEIPs and LDPE/PEIP after the cone calorimeter test

4. Conclusions

A novel oligomeric IFR chelate, Zn-PEIP, containing phosphorus, nitrogen and zinc was synthesized. As a consequence of the multiple coordination positions in Zn-PEIP, the content of zinc ions can be changed to influence the fire retardancy of LDPE/Zn-PEIPs. Study of thermal degradation behaviour for Zn-PEIPs and LDPE/Zn-PEIPs systems reveals that the chelation between PEIP and Zn^{2+} ion can improve the thermal stability of Zn-PEIPs and LDPE; the more Zn^{2+} in the Zn-PEIPs, the better thermal stability of Zn-PEIPs and LDPE. However, there is an optimum content of Zn^{2+} in LDPE/Zn-PEIP according to the LOI and cone calorimetry tests, since the presence of Zn^{2+} adversely affects the intumescent swelling process. More Zn^{2+} in Zn-PEIP may result in less swelling of the char layer. The results showed that the LDPE/Zn-PEIP-0.01 blend had the optimum content of Zn^{2+}, which lead to the formation of the improved protective layer with flexibility and better mechanical properties, giving the lowest value of THR (51MJ/m^2) and the longest value of t_{ign} (160s). Moreover, simultaneous reduction of both THR and residue yield alongside

increase in the ASEA and the yield of CO indicate a gas phase flame retardant effect.

Acknowlegements

The authors thank Mrs. Xiurong Hu of Zhejiang University for the structure-matching study in XRD analysis of the char residue. The authors also greatly acknowledge the financial supports from the National Natural Science Foundation of China (No.51203136), the National Science Foundation of Zhejiang province (No. LQ12E03003) and the Scientific Special Fund of Zhejiang Province (No. 2013C01074).

References

1 Liu, Y.; Cao, Z. H.; Zhang, Y.; Fang, Z. P. Synthesis of Cerium N‑Morpholinomethylphosphonic Acid and Its Flame Retardant Application in High Density Polyethylene. *Ind. Eng. Chem. Res.* **2013**, *52*, 5334.

2 Bourbigot, S.; Duquesne, S. Fire retardant polymers: Recent developments and opportunities. *J. Mater. Chem.* **2007**, *17*, 2283.

3 Wang, D. Y.; Liu, Y.; Ge, X. G.; Wang, Y. Z.; Stec, A. A.; Biswas, B.; Hull, T. R.; Price, D. Effect of metal chelates on the ignition and early flaming behaviour of intumescent fire-retarded polyethylene systems. *Polym. Degrad. Stab.* **2008**, *93*, 1024.

4 Wang, D. Y.; Liu, Y.; Wang, Y. Z.; Perdomo-Artiles, C.; Hull, T. R.; Price, D. Fire retardancy of a reactively extruded intumescent flame retardant polyethylene system enhanced by metal chelates. *Polym. Degrad. Stab.* **2007**, *92*, 1592.

5 Bourbigot, S.; Le Bras, M.; Delobel, R.; Decressain, R.; Amourex, J. P. Synergistic effect of zeolite in an intumescence process: study of the carbonaceous structures using solid-state NMR. *J. Chem. Soc., Faraday Trans.* **1996**, *92*, 149.

6 Lewin, M. Synergism and catalysis in flame retardancy of polymers. *Polym. Adv. Technol.* **2001**, *12*, 215.

7 Braun, U.; Bahr, H.; Sturm, H.; Schartel, B. Flame retardancy mechanisms of metal phosphinates and metal phosphinates in combination with melamine cyanurate in glass-fiber reinforced poly(1,4-butylene terephthalate): the influence of metal cation *Polym. Adv. Technol.* **2008**, *19*, 680.

8 Chen, S. J.; Li, J.; Zhu, Y. K.; Guo, Z. B.; Su, S. P. Increasing the efficiency of intumescent flame retardant polypropylene catalyzed by polyoxometalate based ionic liquid. *J. Mater. Chem. A* **2013**, *1*, 15242.

9 Cao, Z. H.; Zhang, Y.; Song, P. A.; Cai, Y. Z.; Guo, Q.; Fang, Z. P.; Peng, M. A novel zinc chelate complex containing both phosphorus and nitrogen for improving the flame retardancy of low density polyethylene. *J. Anal. Appl. Pyrol.* **2011**, *92*, 339.

10 Li, N.; Xia, Y.; Mao, Z. W.; Wang, L.; Guan, Y.; Zheng, A. Influence of antimony oxide on flammability of polypropylene/intumescent flame retardant system. *Polym. Degrad. Stab.* **2012**, *97*, 1737.

11 Wehner, W. WO 2014060004 A1. April 24, 2014.

12 Wen, X.; Gong, J.; Yu, H. O.; Liu, Z.; Wan, D.; Liu, J.; Jiang, Z. W.; Tang, T. Catalyzing carbonization of poly(L-lactide) by nanosized carbon black combined with Ni_2O_3 for improving flame retardancy. *J. Mater. Chem.* **2012**, *22*, 19974.

13 Hirschler, M. M. Thermal analysis and flammability of polymers Effect of halogen-metal additive systems. *Eur. Polym. J.* **1983**, *19*, 121.

14 Cullis, C. F.; Hirschler, M. M. Char formation from polyolefins. Correlations with low-temperature oxygen uptake and with flammability in the presence of metal halogen systems. *Eur. Polym. J.* **1984**, *20*, 53.

15 Ran, S. Y.; Guo, Z. H.; Chen, C.; Zhao, L. P.; Fang, Z. P. Carbon nanotubes bridged cerium phenylphosphonate hybrids, fabrication and their effects on the thermal stability and flame retardancy of HDPE/BFR composite. *J. Mater. Chem. A* **2014**, *2*, 2999-3007.

16 Li, J. M.; Wilkie, C. A. Improving the thermal stability of polystyrene by Friedel-Crafts chemistry. *Polym. Degrad. Stab.* **1997**, *57*, 293.

17 Wu, N.; Ding, C.; Yang, R. J. Effects of zinc and nickel salts in intumescent flame-retardant polypropylene. *Polym. Degrad. Stab.* **2010**, *95*, 2589.

18 Lewin, M.; Endo, M. Catalysis of intumescent flame retardancy of polypropylene by metallic compounds. *Polym. Adv. Technol.* **2003**,*14*, 3.

19 Jang, J. W.; Kim, J. H.; Bae, J. Y. Effects of Lewis acid-type transition metal chloride additives on the thermal degradation of ABS. *Polym. Degrad. Stab.* **2005**, *88*, 324.

20 Bestaoui, N.; bakhmutova-Albert, E. V.; Rodriguez, A. V.; Llavona, R.; Clearfield, A. Ab-initio Powder Structure Determination of Dichloro[1,2-ethanediylbis(iminomethylene)bis(phosphonato)]trizinc Dihydrate. *Eur. J. Inorg. Chem.* 2005, **2005**, 829.

21 Petersen, H. A. in *Handbook of Fiber Science and Technology.* ed. M. Lewin and S. B. Sello, Dekker: New York, 1983.

22 Chen, X. C.; Ding, Y. P.; Tang, T. Synergistic effect of nickel formate on the thermal and flame-retardant properties of polypropylene. *Polym. Int.* **2005**, *54*, 904.

23 Song, P. A.; Fang, Z. P.; Tong, L. F.; Jin, Y. M.; Lu, F. Z. Effects of metal chelates on a novel oligomeric intumescent flame retardant system for polypropylene. *J. Anal. Appl. Pyrolysis*. **2008**, *82*, 286.

24 Zhang, Y.; Chen, X. L.; Fang, Z. P. Synergistic effects of expandable graphite and ammonium polyphosphate with a new carbon source derived from biomass in flame retardant ABS. *J. Appl. Polym. Sci.* **2013**, *128*, 2424.

25 Schartel, B.; Hull, T. R. Development of fire-retarded materials—Interpretation of cone calorimeter data. *Fire. Mater.* **2007**, *31*, 327.

26 Bee, S. T.; Hassan, A.; Ratnam, C. T.; Tee, T. T.; Sin, L. T.; Hui, D. Dispersion and roles of montmorillonite on structural, flammability, thermal and mechanical behaviours of electron beam irradiated flame retarded nanocomposite. *Compos. Part B-Eng.* **2014**, *61*, 41.

27 Gallina, G.; Bravin, E.; Badalucco, C.; Audisio, G.; Armanini, M.; Chirico, A. D.; Provasoli, F. Application of cone calorimeter for the assessment of class of flame retardants for polypropylene. *Fire. Mater.* **1998**, *22*, 15.

28 Lujan-Acosta, R.; Sánchez-Valdes, S.; Ramírez-Vargas, E.; Ramos-DeValle, L.F.; Espinoza-Martinez, A. B.; Rodriguez-Fernandez, O. S.; Lozano-Ramirez, T.; Lafleur,

P. G. Effect of Amino alcohol functionalized polyethylene as compatibilizer for LDPE/EVA/clay/flame-retardant nanocomposites. *Mater. Chem. Phys.* **2014**, *146*, 437.

29 Gugumus, F. Physico-chemical aspects of polyethylene processing in an open mixer 3. Experimental kinetics of functional group formation. *Polym. Degrad. Stab.* **2000**, *68*, 21

30 Gallo, E.; Schartel, B.; Braun, U.; Russo, P.; Acierno, D. Fire retardant synergisms between nanometric Fe_2O_3 and aluminum phosphinate in poly(butylene terephthalate). *Polym. Adv. Technol.*, **2011**, *22*, 2382.

Table of Contents

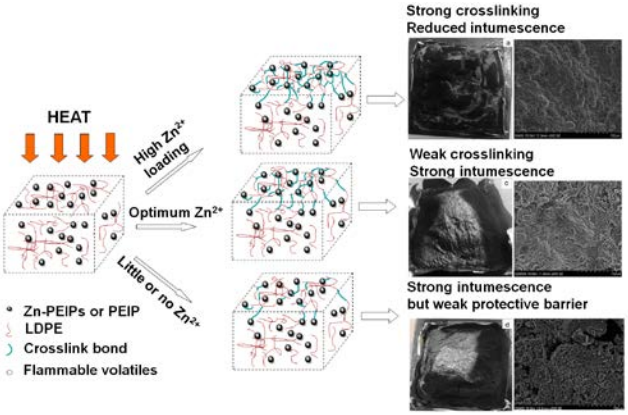

For Table of Contents Only